NANO LETTERS

Letter

pubs.acs.org/NanoLett

How Graphene Islands Are Unidirectionally Aligned on the Ge(110) Surface

Jiayun Dai,[†] Danxia Wang,[‡] Miao Zhang,[†] Tianchao Niu,[†] Ang Li,[†] Mao Ye,[†] Shan Qiao,[†] Guqiao Ding,[†] Xiaoming Xie,[†] Yongqiang Wang,[§] Paul K. Chu,[∥] Qinghong Yuan,*[,†,‡,¶] Zengfeng Di,*[,†] Xi Wang,[†] Feng Ding,[⊥] and Boris I. Yakobson[¶]

[†]State Key Laboratory of Functional Materials for Informatics, Shanghai Institute of Microsystem and Information Technology, Chinese Academy of Sciences, Shanghai 200050, China

[‡]Department of Physics, East China Normal University, Shanghai 200241, China

[§]Materials Science and Technology Division, Los Alamos National Laboratory, Los Alamos, New Mexico 87545, United States

[∥]Department of Physics and Materials Science, City University of Hong Kong, Kowloon, Hong Kong 999077, China

[⊥]Institute of Textiles and Clothing, Hong Kong Polytechnic University, Kowloon, Hong Kong 999077, China

[¶]Department of Materials Science and NanoEngineering, Rice University, Houston, Texas 77005, United States

Supporting Information

ABSTRACT: The unidirectional alignment of graphene islands is essential to the synthesis of wafer-scale single-crystal graphene on Ge(110) surface, but the underlying mechanism is not well-understood. Here we report that the necessary coalignment of the nucleating graphene islands on Ge(110) surface is caused by the presence of step-pattern; we show that on the preannealed Ge(110) textureless surface the graphene islands appear nonpreferentially orientated, while on the Ge(110) surfaces with natural step pattern, all graphene islands emerge coaligned. First-principles calculations and theoretical analysis reveal this different alignment behaviors originate from the strong chemical binding formed between the graphene island edges and the atomic steps on the Ge(110) surface, and the lattice matching at edge-step interface dictates the alignment of graphene islands with the armchair direction of graphene along the [−110] direction of the Ge(110) substrate.

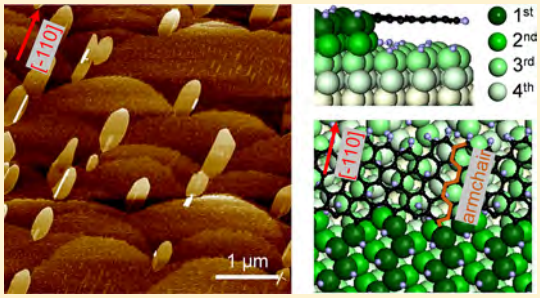

KEYWORDS: *Graphene, alignment, first-principles calculation, surface step, chemical bonding, lattice matching*

Synthesis of single-crystalline monolayer graphene on the wafer scale is essential for realization of its great potential in various fields, especially nanoelectronics.[1−5] Nevertheless, the formation of grain boundaries (GBs) in graphene is almost inevitable in chemical vapor deposition (CVD) growth,[6−9] affecting detrimentally the electronic properties and device performance.[10−12] Besides the efforts to grow graphene from the fewer nuclei,[13−15] the control of the graphene island alignment is also of great importance for eliminating GBs.[16,17] Recently, the most representative demonstration is the CVD synthesis of wafer-size single-crystalline graphene on Ge(110) surface via the seamless stitching of unidirectionally aligned graphene islands.[18] However, the underlying mechanism that governs the alignment of graphene island has not been well understood despite of the experimental success. It was proposed that the anisotropic 2-fold symmetry of the Ge(110) surface was responsible for the unidirectional alignment of graphene islands.[18] However, in addition to the observation of uniaxial alignment, graphene islands with nonpreferential orientations can also be observed on a preannealed Ge(110) surface (see methods in the Supporting Information) without altering the C_2 symmetry of the substrate surface, as shown in Figure 1a,b. This observation expressly suggests that the anisotropic 2-fold symmetry of the Ge(110) substrate may not be the determinative factor orientating the graphene islands.[18,19]

Herein, by conducting a series of experiments and first-principles density functional theory (DFT) calculations, we reveal that, in addition to the crystalline symmetry of the Ge(110) substrate, the atomic steps on the Ge(110) surface and lattice matching between such atomic step and graphene edge are crucial for the unidirectional alignment of graphene islands. All of the unidirectionally aligned graphene islands are attached to the atomic steps on the Ge(110) surface with the armchair directions of the graphene islands always along the [−110] direction of Ge(110) substrate, independent of the direction of the atomic steps. DFT calculation and theoretical analysis reveal that graphene islands are attached to the atomic

Received: February 3, 2016
Revised: April 19, 2016
Published: April 21, 2016

ACS Publications © 2016 American Chemical Society

DOI: 10.1021/acs.nanolett.6b00486
Nano Lett. 2016, 16, 3160−3165

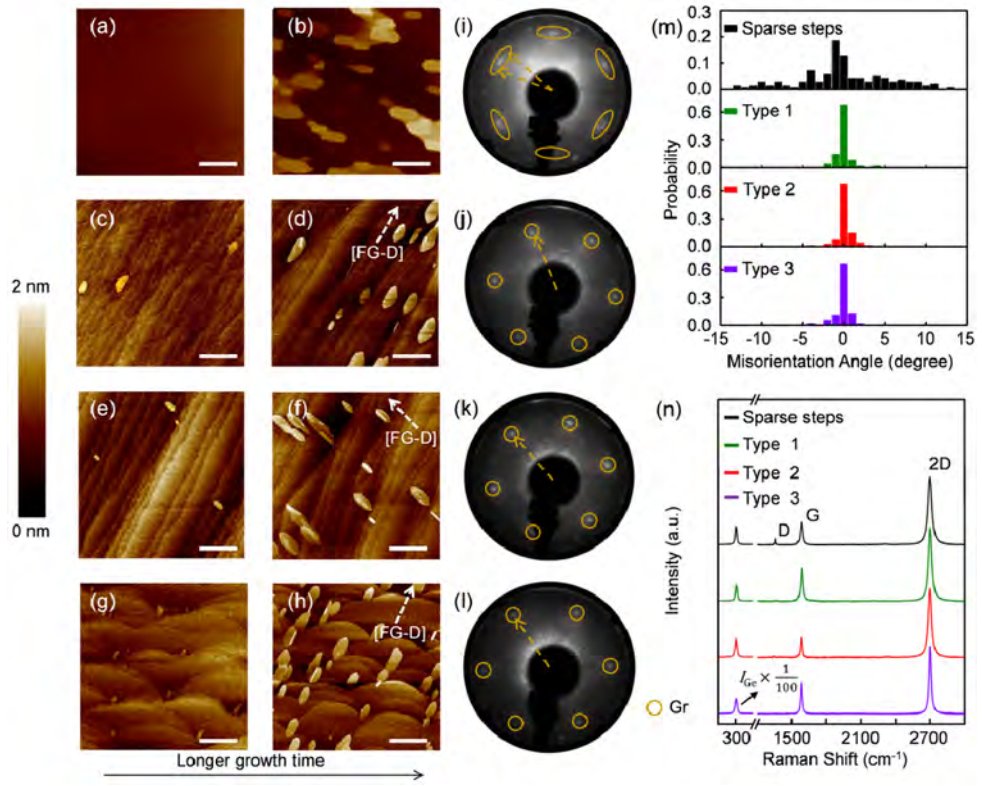

Figure 1. (a) AFM images of the preannealed Ge(110) surface with a reduced density of atomic steps. (b) AFM images of the graphene islands with multiple orientations grown on the preannealed Ge(110) surface with a reduced density of atomic steps. (c,d) AFM images of well-aligned graphene islands produced on the Ge(110) surface with type 1 atomic steps. (e,f) AFM images of well-aligned graphene islands fabricated on the Ge(110) surface with type 2 atomic steps. (g,h) AFM images of well-aligned graphene islands prepared on the Ge(110) surface with type 3 atomic steps. The FG-D of the well-aligned graphene islands is indicated by dashed white arrow. (i–l) LEED patterns of graphene grown on the Ge(110) surfaces with a reduced density of atomic steps and three typical atomic steps, respectively. The solid orange circles denote the diffraction spots of graphene (Gr) islands. (m) Histogram of misorientation-angles with respect to the FG-D of graphene islands prepared on the Ge(110) substrates with a reduced density of atomic steps and three typical atomic steps. (n) Raman spectra of the continuous graphene film directly grown on the Ge(110) substrates with a reduced density of atomic steps and three typical atomic steps. The scale bars in a–h are 1 μm.

steps of the Ge(110) surface by strong chemical bonds, and the lattice matching between graphene edge and the crystal lattice of the Ge(110) surface dictates the alignment of the graphene islands.

Figure 1c–h presents a series of atomic force microscopy (AFM) images showing the evolution of graphene islands on the Ge(110) surfaces with three typical atomic steps. It should be noted that, for the commercially available substrates, perfect flat surfaces are rare and most substrate surfaces consist of flat terraces separated by numerous atomic steps, which are primarily controlled by the wafer manufacturing process including slicing, grinding, and polishing. All graphene islands on the stepped Ge(110) surface attach exclusively to the atomic steps from nucleation (Figure 1c,e,g), and the attachment is preserved as growth continues and the island size increases (Figure 1d,f,h). Each graphene island appears as a leaf-like shape with the long-axis along the "fast growth-direction" (FG-D). On the stepped Ge(110) surfaces, regardless the direction of atomic steps, the FG-Ds of all graphene islands are almost aligned to the same direction. In Figure 1c,d, the FG-Ds of the leaf-like islands are roughly along the direction of the atomic steps, while nearly perpendicular to the direction of the surface steps in Figure 1e,f. Unlike the two former samples whose steps are macroscopically straight, atomic steps shown in Figure 1g,h are in sector-like shape with many kinks. On this kind of stepped surface, nearly all the graphene islands are attached to the kink site with the FG-Ds along the direction of the bisectors of the kinks. And, even for the atomic steps with other irregular shapes, the FG-Ds of graphene islands always follow the same direction (Supporting Information, Figure S1). For further evidence, the low-energy electron diffraction (LEED) pattern of the graphene islands prepared on each stepped Ge(110) surface reveals six hexagonally arranged spots, which corresponds to unidirectional alignment of the islands (Figure 1j–l). However, as the density of the atomic steps on the Ge(110) surface is reduced by preannealing (Figure 1a), the graphene islands grown under the same experimental condition are no longer unidirectionally aligned (Figure 1b) but instead have multiple orientations with the misorientation-angles varying between −12° and 12°, which are distinct from those formed on Ge(110) with normal density of atomic steps (Figure 1m). Be noted that the flow rate of H_2 for preannealed and pristine Ge substrates were varied to obtain graphene islands with adequate density for better orientation statistics (see methods in the Supporting Information). The azimuthally elongated diffraction spots in the LEED pattern also indicate that these graphene islands have various orientations (Figure 1i). The graphene islands with the unidirectional alignment are able to seamlessly merge to form the single-crystalline graphene film without grain boundary defects (Figure 1n). In contrast, nonaligned graphene islands, which are formed on preannealed Ge(110) textureless surface, lead to the incommensurate stitching as they coalesce

DOI: 10.1021/acs.nanolett.6b00486
Nano Lett. 2016, 16, 3160–3165

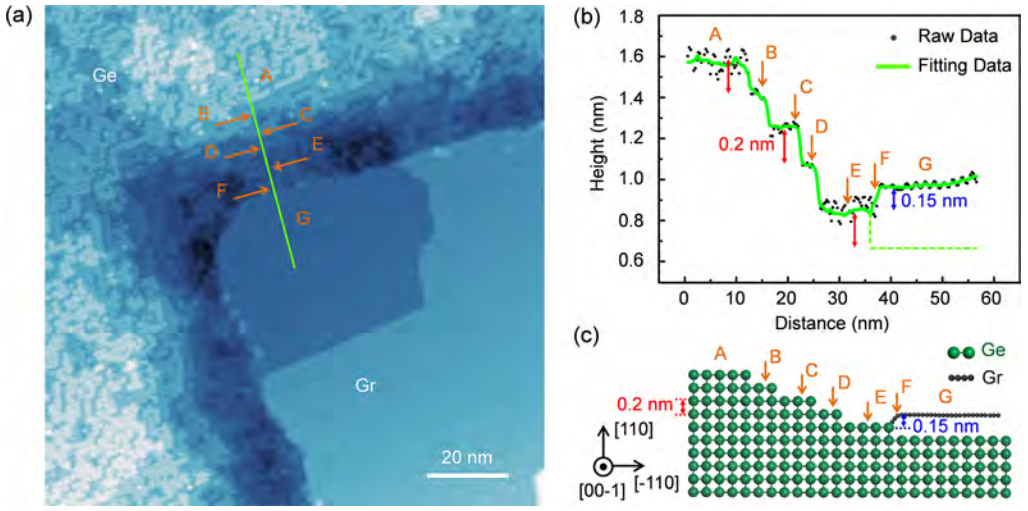

Figure 2. (a) High resolution STM image of graphene island attached to the atomic step on Ge(110) surface (V = 2.2 V, I = 0.5 A). (b) Height profile measured along the solid green line AG marked in a. (c) Sketch drawing of atomic structure of graphene island attached to the atomic step. The dark green ball and black ball represents Ge atom and graphene atom, respectively.

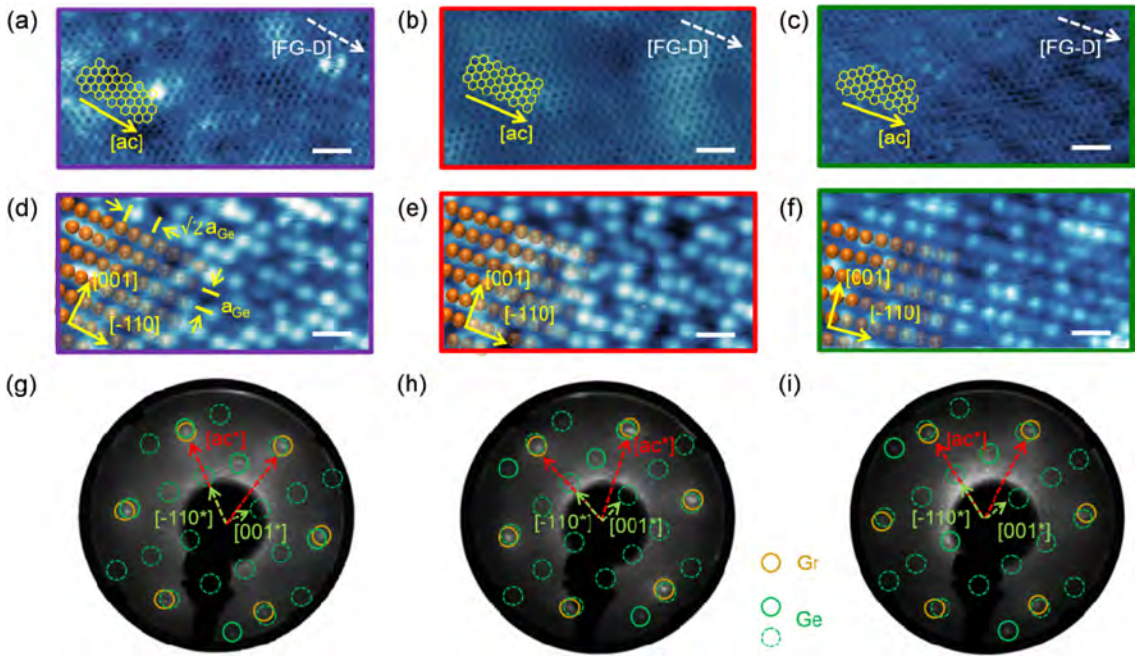

Figure 3. (a–c) High-resolution STM images of the honeycomb graphene structure acquired from the graphene islands near three representative stepped surfaces at a low voltage (V = −0.2 V). The atomic structure of graphene is overlaid. Meanwhile, the solid yellow arrow and dashed white arrow indicate the armchair direction of graphene and FG-D of the graphene island, respectively. (d–f) High resolution STM images showing the lattice structure of the Ge(110) plane at a high voltage (V = −1.0 V). The orange balls are superimposed to demonstrate the germanium atoms. Scale bars in (a–f) are 1 nm. The tunneling currents are (a) 0.5 nA, (b) 1.5 nA, (c) 1.0 nA, (d) 2 nA, (e) 0.2 nA, and (f) 0.5 nA, respectively. (g–i) LEED patterns for graphene islands on three representative stepped Ge(110) surfaces. The outer six diffraction spots highlighted by the solid orange circles are associated with the graphene (Gr), whereas the additional diffraction spots highlighted by the solid (observed) or dotted (derived) green circles are ascribed to Ge(110) substrate (Ge). The reciprocal lattice vectors of graphene and (110) plane of the Ge substrate are indicated by dashed red and green arrows, respectively.

to form a continuous film. Therefore, extended grain boundary defects are inevitably formed (Figure 1n).

In Figure 2a–c, we present the direct evidence showing the gapless attachment between graphene island and the atomic steps on the Ge(110) surface. Scanning tunneling microscopy (STM) image of a graphene island attached to the atomic step is shown in Figure 2a. A height profile shown in Figure 2b displays that the height difference between point AB, BC, CD, and DE is equal to 0.2 nm without exception, which corresponds to single atomic step for Ge(110) surface. However, the height of graphene island (F in Figure 2a) differs from that of neighboring Ge terrace (E in Figure 2a) by 0.15 nm, and such a measured value could be overestimated considering the semimetal/semiconductor nature of graphene/Ge as the electronic density of states (DOS) is convoluted with the surface geometry in a STM topography. Therefore, the actual height difference could be quite close to the theoretical height difference (0.135 nm) between Ge atomic step (0.2 nm)

DOI: 10.1021/acs.nanolett.6b00486
Nano Lett. 2016, 16, 3160–3165

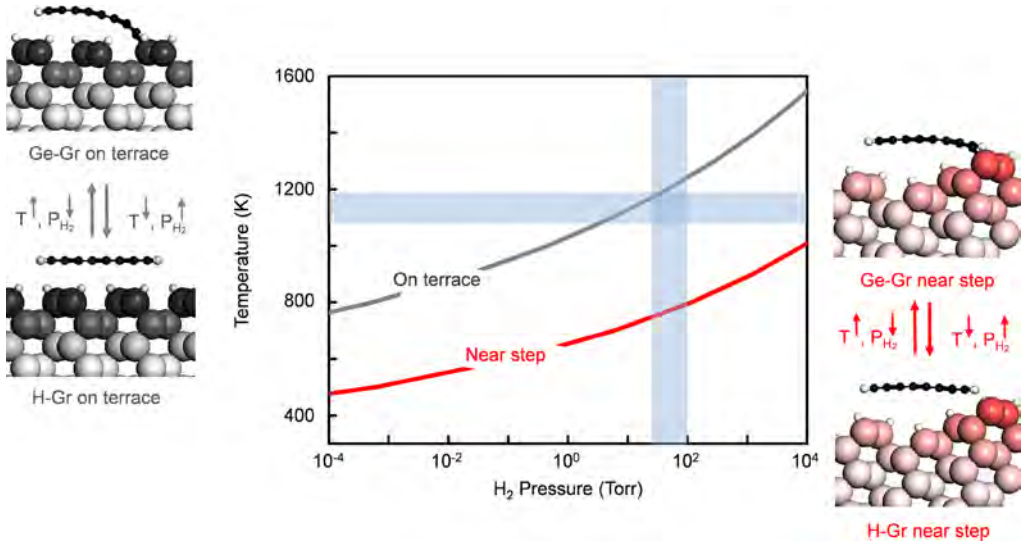

Figure 4. Thermodynamic diagrams of graphene with the armchair edge on the Ge(110) surface with terraces or [−110] oriented steps. Structures for H- and Ge-passivated graphene with armchair edge on the terrace are shown in the left panel, and those near the [−110] oriented atomic step are shown in the right panel.

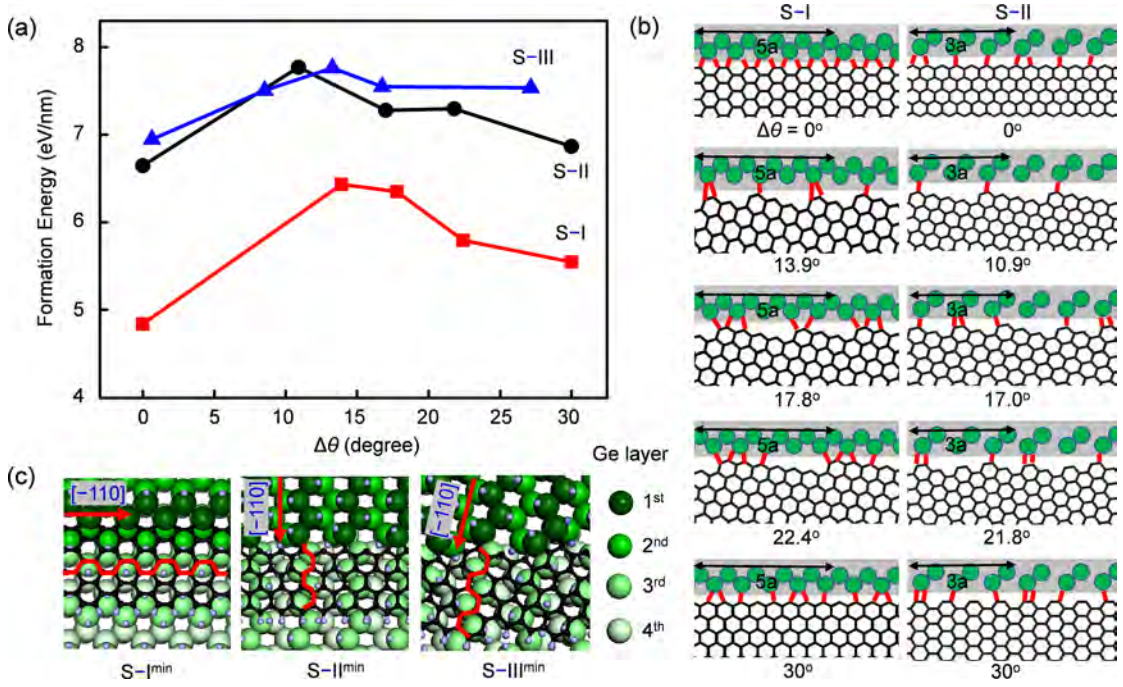

Figure 5. (a) Formation energies of the Ge-Gr interfaces formed at the three typical steps on the Ge(110) surface as a function of the edge deflection angle Δθ. (b) Illustration of the chemical bonding at the Ge-Gr interface for the different graphene islands with different Δθ relative to S−I ([−110] oriented step) and S−II ([001] oriented step). (c) Most stable structures of the Ge-Gr interfaces formed at three types of steps: [−110] oriented step (S−I^{min}), [001] oriented step (S−II^{min}), and the step with an arbitrary direction (S−III^{min}). The [−110] direction on the Ge(110) surface and the armchair direction of graphene are indicated by the red arrow and red curve, respectively.

and monolayer graphene (0.335 nm).[20] Thus, it can be concluded that the graphene island is seamlessly attached to the atomic step on Ge(110) surface as observed by AFM measurements above. Besides, the sketch of the proposed model revealing the structure of graphene island attached to the atomic step of Ge(110) surface is shown in Figure 2c.

To further elucidate the orientation of the graphene islands on the stepped Ge(110) substrate at the atomic scale, STM measurement is further performed on graphene islands near three representative stepped surfaces (Figure S2). By varying the tunneling voltage, the lattice structures of the top graphene and underlying substrate can be revealed alternatively. At a tunneling bias of −0.2 V (Figure 3a−c), a clear honeycomb pattern of monolayer graphene is observed. As the tunneling voltage is increased to −1.0 V (Figure 3d−f), the honeycomb pattern of graphene vanishes and the crystal lattice of the Ge(110) face appears due to the transparency of the graphene layer at the tunneling energy well above or well below the Fermi surface (E_F).[21,22] Although the complete periodicity of the lattice structure cannot be clearly seen due to the

DOI: 10.1021/acs.nanolett.6b00486
Nano Lett. 2016, 16, 3160−3165

complicated pattern of the H terminated Ge surface,[18] it is still feasible to distinguish the [001] and [−110] directions of the Ge(110) substrate, as marked in Figure 3d−f. By comparing the lattice images, it can be concluded that the armchair direction of the graphene lattice coincides with the [−110] direction of the Ge(110) substrate, and both directions are parallel to the FG-D of graphene island. The detailed analysis of LEED patterns (Figure 1j−l) further confirms that the graphene islands are well-aligned macroscopically, and the armchair direction of the graphene lattice is along the [−110] direction of the Ge(110) substrate, as illustrated in Figure 3g−i.

To understand why graphene islands on stepped Ge(110) surfaces have unidirectional alignment but their orientations on the preannealed Ge(110) surface are widely distributed, DFT calculation and thermodynamic analysis are carried out to compare the chemical interactions of graphene island edges to atomic steps and flat terrace (see Supporting Information). Figure 4 shows the structures and thermodynamic diagram of graphene with the armchair edge on the terraces or near the typical [−110] oriented steps of Ge(110) surface. It is observed that the graphene island edge on the terrace or near the atomic step can be either terminated by hydrogen (H-Gr) or passivated by the Ge substrate (Ge-Gr) during the CVD growth, depending on the temperature and partial pressure of H_2 in the carrier gas.[23,24] Our calculation results demonstrate that, on the terrace of Ge(110), the H-Gr structure is more favorable than the Ge-Gr one under the typical growth conditions in our experiment (shown by the overlapping blue zone in the thermodynamic diagram in Figure 4, where $T \sim$ 1100−1200 K and $P_{H_2} \sim$ 50−100 Torr). However, in the vicinity of the atomic steps, the Ge-Gr structure is more stable under the similar growth conditions. The thermodynamic diagrams of graphene with the zigzag edge on terraces or near typical [001] oriented steps of Ge(110) surface are quite similar to those of the armchair edges (Supporting Information, Figure S3), so the termination behavior of graphene island edge is similar. Therefore, it can be concluded that graphene islands are hydrogen-passivated on the terrace, but step-terminated near the atomic step. For graphene islands on the terrace of Ge(110) surface, hydrogen termination of the edge impedes the formation of strong chemical bonding between graphene and Ge(110) substrate and thus only weak van der Waals (vdW) interaction exists, which is unable to strictly control the alignment of graphene islands. Therefore, if the density of atomic steps on the Ge(110) surface is reduced significantly by preannealing, the graphene islands have fewer chance to attach to the atomic steps but to interact with the terrace of Ge(110) surface via weak vdW force. This leads to less control on the alignment of graphene islands (Figure 1a,b). However, for commercial Ge(110) substrate with usual density of atomic steps, graphene islands prefer to attach to the atomic step of Ge(110) via strong chemical bonding (Figure 2a), so Ge-terminated graphene edge is expected with the desorption of H_2 moleculars.

To elucidate how C−Ge chemical bonds formed between atomic steps and graphene edges dictate the unidirectional alignment of graphene islands, we calculate the formation energies of the graphene edge bonded to three typical steps as a function of the edge deflection angle $\Delta\theta$ (Figure 5a and Supporting Information, Figure S4), where $\Delta\theta$ is defined as the misorientation angle between the armchair direction of graphene and [−110] direction of the Ge(110) surface. For the [−110] oriented step on the Ge(110) surface (S−I in Figure 5a), the formation energy of the Ge-Gr interface increases from 4.84 to 6.43 eV/nm as $\Delta\theta$ changes from 0 to 13.9°. With further increase of $\Delta\theta$ until 30°, the formation energy decreases gradually but is still above the minimum obtained at $\Delta\theta$ = 0. As the formation energy is closely correlated with the chemical bonds at the Ge-Gr interface, the number of C−Ge bonds formed between the graphene edge and atomic step changes accordingly as shown in Figure 5b. And, the maximum number of C−Ge bonds is obtained for $\Delta\theta$ = 0, which corresponds to the alignment that the armchair direction of the graphene is parallel to the [−110] direction of the Ge(110) surface as demonstrated by S−I^{min} in Figure 5c. In this situation, all the carbon atoms distributed along the graphene edge can form covalent bonds with [−110] oriented atomic step of the Ge(110) substrate, and coherent lattice matching occurs due to the approximate lattice parameters along the two directions. With respect to other graphene edges with certain deflection angles from the armchair direction, there are always some nonpassivated carbon atoms along the graphene edge, and hence higher formation energy is expected as shown in Figure 5a. With regard to the zigzag edge bonding with the [001] oriented steps, i.e., S−II on the Ge(110) substrate, the case is quite similar to the armchair edge's bonding at the [−110] oriented step, and the minimum formation energies are obtained at $\Delta\theta$ = 0 as well (S−II^{min} in Figure 5c).

For any other atomic steps with a deviation angle of χ in relative to [−110] oriented step ($0° < \chi < 90°$), the formation energy of graphene edge on the atomic step can be expressed analytically from the edge formation energies on the basic [−110] and [001] oriented step $\gamma(\chi) \sim \gamma_{[-110]}(\Delta\theta)\cos(\chi) + \gamma_{[001]}(\Delta\theta)\sin(\chi)$, in which $\gamma_{[-110]}(\Delta\theta)$ and $\gamma_{[001]}(\Delta\theta)$ are the formation energies of graphene edges on [−110] and [001] oriented steps, respectively. As both $\gamma_{[-110]}(\Delta\theta)$ and $\gamma_{[001]}(\Delta\theta)$ have the minimum at $\Delta\theta$ = 0, $\gamma(\chi)$ also has the minimum when $\Delta\theta$ = 0. This demonstrates that, for graphene edge bonded to the atomic step with any arbitrary rotation angle, the minimum formation energy always appears at $\Delta\theta$ = 0. Such a conclusion is further supported by our direct DFT calculations, i.e., S−III on the Ge(110) substrate, the minimum formation energy of graphene edge is achieved at $\Delta\theta$ = 0 as well (Figure 5a). Therefore, regardless of the direction of the atomic step, the graphene island which attaches to the atomic step to form the energetically favorable Ge-Gr interface should possess invariable alignment on the Ge(110) surface. With such alignment, the armchair direction of graphene island is always parallel to the [−110] direction of Ge(110) surface, as demonstrated by S−III^{min} in Figure 5c.

In conclusion, we show the preferential attachment of graphene islands to the atomic steps on the Ge(110) substrate, and graphene islands attached to steps are uniaxially aligned with their armchair directions parallel to the [−110] direction of the Ge(110) substrate independent of the direction of atomic steps. First-principles calculation elucidates that the unidirectional alignment of graphene islands is attributed to lattice matching at the interface where strong chemical bonds are formed between the graphene edge and atomic step. Our study provides a deep insight into the role of atomic steps on the alignment of graphene islands, which may substantially promote single crystal graphene wafer engineering, thus enabling the veritable integration of graphene into the current semiconducting technology.

DOI: 10.1021/acs.nanolett.6b00486
Nano Lett. 2016, 16, 3160−3165

■ ASSOCIATED CONTENT

Supporting Information

The Supporting Information is available free of charge on the ACS Publications website at DOI: 10.1021/acs.nanolett.6b00486.

Experimental methods, AFM images and DFT calculations for phase diagram calculation, formation energy of the Ge-Gr interface (PDF)

■ AUTHOR INFORMATION

Corresponding Authors

*E-mail: zfdi@mail.sim.ac.cn.

*E-mail: qhyuan@rice.edu.

Author Contributions

J.D. and D.W. contributed equally. Z.D. and X.W. supervised the project. Z.D., M.Z., X.X., and J.D. conceived and designed the experiments. Z.D., G.D., and J.D. synthesized the graphene samples and carried out AFM and Raman measurements. T.N. and A.L. performed the STM measurements. M.Y. and S.Q. performed the LEED measurements. Q.Y., D.W., and F.D. performed the DFT calculation. Z.D., Q.Y., F.D., P.K.C., Y.W., J.D., and B.Y. analyzed the data and cowrote the paper. All the authors discussed the results and commented on the manuscript.

Notes

The authors declare no competing financial interest.

■ ACKNOWLEDGMENTS

This work was financially supported by Creative Research Groups of National Natural Science Foundation of China (No. 61321492), National Science and Technology Major Project (Grant No. 2011ZX02707), National Natural Science Foundation of China under Grant (Nos. 21303056 and 61274136) and Shanghai Pujiang Program (13PJ1402600). Partial support was also provided by the Center for Integrated Nanotechnologies (CINT) and US DOE nanoscience user facility jointly operated by Los Alamos and Sandia National Laboratories, City University of Hong Kong Applied Research Grant (ARG) No. 9667104, Guangdong - Hong Kong Technology Cooperation Funding Scheme (TCFS) GHP/015/12SZ.

■ REFERENCES

(1) Castro Neto, A. H.; Guinea, F.; Peres, N. M. R.; Novoselov, K. S.; Geim, A. K. *Rev. Mod. Phys.* **2009**, *81*, 109−162.

(2) Avouris, P. *Nano Lett.* **2010**, *10*, 4285−4294.

(3) Das Sarma, S.; Adam, S.; Hwang, E. H.; Rossi, E. *Rev. Mod. Phys.* **2011**, *83*, 407−470.

(4) Gan, X.; Shiue, R.-J.; Gao, Y.; Meric, I.; Heinz, T. F.; Shepard, K.; Hone, J.; Assefa, S.; Englund, D. *Nat. Photonics* **2013**, *7*, 883−887.

(5) Mics, Z.; Tielrooij, K.-J.; Parvez, K.; Jensen, S. A.; Ivanov, I.; Feng, X.; Mullen, K.; Bonn, M.; Turchinovich, D. *Nat. Commun.* **2015**, *6*, 7655.

(6) Yu, Q.; Jauregui, L. A.; Wu, W.; Colby, R.; Tian, J.; Su, Z.; Cao, H.; Liu, Z.; Pandey, D.; Wei, D.; Chung, T. F.; Peng, P.; Guisinger, N. P.; Stach, E. A.; Bao, J.; Pei, S.-S.; Chen, Y. P. *Nat. Mater.* **2011**, *10*, 443−449.

(7) Guo, W.; Wu, B.; Li, Y.; Wang, L.; Chen, J.; Chen, B.; Zhang, Z.; Peng, L.; Wang, S.; Liu, Y. *ACS Nano* **2015**, *9*, 5792−5798.

(8) Rasool, H. I.; Ophus, C.; Klug, W. S.; Zettl, A.; Gimzewski, J. K. *Nat. Commun.* **2013**, *4*, 2811.

(9) Duong, D. L.; Han, G. H.; Lee, S. M.; Gunes, F.; Kim, E. S.; Kim, S. T.; Kim, H.; Ta, Q. H.; So, K. P.; Yoon, S. J.; Chae, S. J.; Jo, Y. W.; Park, M. H.; Chae, S. H.; Lim, S. C.; Choi, J. Y.; Lee, Y. H. *Nature* **2012**, *490*, 235−239.

(10) Fei, Z.; Rodin, A. S.; Gannett, W.; Dai, S.; Regan, W.; Wagner, M.; Liu, M. K.; McLeod, A. S.; Dominguez, G.; Thiemens, M.; Castro Neto, A. H.; Keilmann, F.; Zettl, A.; Hillenbrand, R.; Fogler, M. M.; Basov, D. N. *Nat. Nanotechnol.* **2013**, *8*, 821−825.

(11) Tsen, A. W.; Brown, L.; Levendorf, M. P.; Ghahari, F.; Huang, P. Y.; Havener, R. W.; Ruiz-Vargas, C. S.; Muller, D. A.; Kim, P.; Park, J. *Science* **2012**, *336*, 1143−1146.

(12) Huang, P. Y.; Ruiz-Vargas, C. S.; van der Zande, A. M.; Whitney, W. S.; Levendorf, M. P.; Kevek, J. W.; Garg, S.; Alden, J. S.; Hustedt, C. J.; Zhu, Y.; Park, J.; McEuen, P. L.; Muller, D. A. *Nature* **2011**, *469*, 389−392.

(13) Hao, Y.; Bharathi, M. S.; Wang, L.; Liu, Y.; Chen, H.; Nie, S.; Wang, X.; Chou, H.; Tan, C.; Fallahazad, B.; Ramanarayan, H.; Magnuson, C. W.; Tutuc, E.; Yakobson, B. I.; McCarty, K. F.; Zhang, Y.-W.; Kim, P.; Hone, J.; Colombo, L.; Ruoff, R. S. *Science* **2013**, *342*, 720−723.

(14) Wu, T.; Zhang, X.; Yuan, Q.; Xue, J.; Lu, G.; Liu, Z.; Wang, H.; Wang, H.; Ding, F.; Yu, Q.; Xie, X.; Jiang, M. *Nat. Mater.* **2015**, *15*, 43−47.

(15) Li, X. S.; Magnuson, C. W.; Venugopal, A.; Tromp, R. M.; Hannon, J. B.; Vogel, E. M.; Colombo, L.; Ruoff, R. S. *J. Am. Chem. Soc.* **2011**, *133*, 2816−2819.

(16) Zhang, X. Y.; Xu, Z. W.; Hui, L.; Xin, J.; Ding, F. *J. Phys. Chem. Lett.* **2012**, *3*, 2822−2827.

(17) Yuan, Q.; Yakobson, B. I.; Ding, F. *J. Phys. Chem. Lett.* **2014**, *5*, 3093−3099.

(18) Lee, J.-H.; Lee, E. K.; Joo, W.-J.; Jang, Y.; Kim, B.-S.; Lim, J. Y.; Choi, S.-H.; Ahn, S. J.; Ahn, J. R.; Park, M.-H.; Yang, C.-W.; Choi, B. L.; Hwang, S.-W.; Whang, D. *Science* **2014**, *344*, 286−289.

(19) Artyukhov, V. I.; Hao, Y.; Ruoff, R. S.; Yakobson, B. I. *Phys. Rev. Lett.* **2015**, *114*, 115502.

(20) Lee, C.; Wei, X.; Kysar, J. W.; Hone, J. *Science* **2008**, *321*, 385−388.

(21) Brar, V. W.; Zhang, Y.; Yayon, Y.; Ohta, T.; McChesney, J. L.; Bostwick, A.; Rotenberg, E.; Horn, K.; Crommie, M. F. *Appl. Phys. Lett.* **2007**, *91*, 122102.

(22) Rutter, G. M.; Guisinger, N. P.; Crain, J. N.; Jarvis, E. A. A.; Stiles, M. D.; Li, T.; First, P. N.; Stroscio, J. A. *Phys. Rev. B: Condens. Matter Mater. Phys.* **2007**, *76*, 235416.

(23) Shu, H.; Chen, X.; Ding, F. *Chem. Sci.* **2014**, *5*, 4639−4645.

(24) Zhang, X.; Wang, L.; Xin, J.; Yakobson, B. I.; Ding, F. *J. Am. Chem. Soc.* **2014**, *136*, 3040−3047.

DOI: 10.1021/acs.nanolett.6b00486
Nano Lett. 2016, 16, 3160−3165

Supporting Information for

How Graphene Islands Are Unidirectionally Aligned on the Ge(110) surface

Jiayun Dai,[†,#] Danxia Wang,[‡,#] Miao Zhang,[†] Tianchao Niu,[†] Ang Li,[†] Mao Ye,[†] Shan Qiao,[†] Guqiao Ding,[†] Xiaoming Xie,[†] Yongqiang Wang,[§] Paul K. Chu,[‖] Qinghong Yuan,[*,‡,¶] Zengfeng Di,[*,†] Xi Wang,[†] Feng Ding,[⊥] and Boris I. Yakobson[¶]

[†]State Key Laboratory of Functional Materials for Informatics, Shanghai Institute of Microsystem and Information Technology, Chinese Academy of Sciences, Shanghai 200050, China

[‡]Department of Physics, East China Normal University, Shanghai 200241, China

[§]Materials Science and Technology Division, Los Alamos National Laboratory, Los Alamos, New Mexico 87545, United States

[‖]Department of Physics and Materials Science, City University of Hong Kong, Kowloon, Hong Kong 999077, China

[⊥]Institute of Textiles and Clothing, Hong Kong Polytechnic University, Kowloon, Hong Kong 999077, China

¶Department of Materials Science and NanoEngineering, Rice University, Houston, Texas 77005, United States.

#These authors contributed equally to this work.

*Corresponding Author: qhyuan@rice.edu, zfdi@mail.sim.ac.cn.

Methods

Graphene synthesis. The Ge(110) substrates (500 μm thick, AXT) were cut into 1×1 cm^2 pieces and placed in a 2-inch horizontal quartz tube. The quartz tube was evacuated to approximately 10^{-4} mbar and then filled with 200 standard cubic cm per min (sccm) argon (Ar, 99.9999% purity) and hydrogen (H_2, 99.9999% purity). To synthesize the graphene islands with adequate density, H_2 gas flow rate of 25 sccm was chosen for pre-annealed Ge substrate (flat surface). While, for graphene grown on Ge substrate with type 1, type 2 and type 3 atomic steps (rough surface), H_2 gas flow rates were selected as 30 sccm, 30 sccm and 27 sccm, respectively. Then the quartz tube was heated to 910 °C for 30 min and 0.5 sccm methane (CH_4, 99.99%) was introduced to deposit the graphene film for different durations (from 60 min to 200 min). Afterwards, the CH_4 gas was turned off and the furnace was cooled to room temperature under flowing H_2 and Ar. The step-terrace structure was primarily determined by the unavoidable cutting misalignments with respect to the (110) plane when the crystal surfaces were prepared,[1] and it was found that the atomic step density on Ge(110) surface was relatively stable at the growth temperature of 910 ^oC, but decreased with the increase of temperature. When the annealing temperature approached to the melting point of Ge (938.3 ^oC), the atomic steps on the Ge(110) surface were dramatically reduced. In order to reduce the density of the atomic steps, the Ge(110) substrate was intentionally pre-annealed at 937 ^oC (close to the melting point of Ge) for at least 30 min under flowing H_2 and Ar.

Characterization. The topological images of graphene were obtained by the AFM (Multimode 8,

Bruker) in the tapping mode using RTESP AFM tips. Raman spectroscopy (HORIBA Jobin Yvon HR800) was performed using an Ar^+ laser with a wavelength of 514 nm and a spot size of 1 μm. Scanning tunneling microscopy (SPECS JT-STM) was performed in an ultrahigh vacuum (UHV) chamber with a base pressure below 8×10^{-11} mbar at 4.3 K. The STM measurements were taken in the constant current mode by applying a bias voltage to the sample. The LEED measurements were conducted on a 6-inch LEED apparatus (ErLEED 100, SPECS GmbH) in ultrahigh vacuum (base pressure < 5×10^{-8} Pa). The electron beam energy was set to 130 eV for all the samples and the diameter of the electron beam was ~1 mm.

Computational details. The calculation was performed within the framework of DFT as implemented in the Vienna Ab initio Simulation Package (VASP). The electronic exchange and correlation were included through the generalized gradient approximation (GGA) in the Perdew-Burke-Ernzerhof (PBE) form. The interaction between valence electrons and ion cores was described by the projected augmented wave (PAW) method and the energy cutoff for the plane wave functions was 400 eV. The van der Waals interaction was considered by using DFT-D_2 and the spin-polarized calculation was performed for dangling bonds on the graphene edge. All the structures were optimized until the maximum force component on each atom was less than 0.02 eV/Å. The vacuum layer inside the super-cell was kept as large as 15 Å to avoid the interaction between adjacent unit cells. For a supercell larger than 15 Å× 15 Å× 15 Å，the Brillouin zone was sampled only by the G point, otherwise a 2×1×1 or 1×5×1 k-point mesh was used. The substrate was modeled as a periodic slab consisting of at least five atomic layers and

the bottom two layers were fixed to mimic the bulk. Restricted by the calculation size, the substrate lattice was stretched or compressed slightly (< 4 %) to build a co-periodic lattice for graphene and substrate. The Ge atoms on the top and bottom layers were passivated by H atoms.

Phase diagram calculation

The optimized geometries and formation energies of hydrogen and germanium passivated graphene nanoribbons with armchair (AC-GNR) edges on the flat and stepped Ge(110) surfaces (shown in Figure 4) were calculated. A [-110] oriented step was chosen as a typical atomic step on the Ge(110) surface. The H terminated AC-GNR was put on the substrate with the armchair edge along the [-110] direction of the Ge(110) surface. By interacting with the H-passivated Ge(110) surface, some of the H atoms in the graphene edge would react with the H atoms on the substrate and were desorbed as H_2. To compare the stability of the four structures, we defined the formation energy, E_f, of each structure as:

$$E_f = (E_{(tot)} + 0.5\Delta n \times E_{(H_2)} - E_{(sub)} - E_{(GNR-H)}) / L \qquad (1)$$

where the $E_{(tot)}$ are the energies of the four structures shown in Figure 4, $E_{(H_2)}$ is the energy of hydrogen molecule, $E_{(sub)}$ and $E_{(GNR\text{-}H)}$ are the energies of Ge(110) substrate and H-terminated graphene nanoribbons (GNR-H), respectively, Δn is the number of H_2 molecule dehydrogenated from C−Ge bond formation, and L is the length of supercell along the periodic direction. The two structures on the left panel of Figure 4 represent the hydrogen-passivated graphene (H-Gr) edge and germanium-passivated graphene (Ge-Gr) edge on the flat terrace of the Ge(110) surface and

the structures with the H-Gr and Ge-Gr edges near the [-110] oriented step of the Ge(110) surface are shown in the right panel of Figure 4.

To obtain the thermodynamic phase diagram of AC-GNR on the Ge(110) surface, it is essential to compare the free-energy difference ΔG of AC-GNR with Ge-Gr and H-Gr structures. ΔG can be calculated by:

$$\Delta G = \Delta E_f - N_H \times \mu_H(T, P) \qquad (2)$$

where ΔE_f is the difference in the formation energy (calculated by Eq. 1) between the H-Gr and the Ge-Gr edges, N_H is the number of H atoms, and μ_H is the chemical potential of the H_2 gas as a function of H_2 partial pressure P and temperature T. By setting $\Delta G = 0$, we could obtain the thermodynamic diagram of graphene with the armchair edge on the Ge(110) surface with terraces or [-110] oriented steps as shown in Figure 4. Meanwhile, the similar thermodynamic diagram of graphene with the zigzag edge was obtained and shown in Supporting Information Figure S3.

Formation energy of the Ge-Gr interface

Three typical surface steps were considered in our calculation: [-110] oriented step (S-I), [001] oriented step (S-II), and step with an arbitrary direction (76.74° deviated from [-110] direction, S-III). The GNR with one edge terminated by H atoms and another bare edge attached to the atomic step of Ge(110) surface was put near the step edge and optimized. To explore the optimum bonding orientation of the graphene edge at each surface step, we calculated the

formation energies of the Ge-Gr edge with different $\Delta\theta$ which was defined as the misorientation angle between the [-110] direction of the Ge(110) surface and the armchair direction of graphene. The formation energy of Ge-Gr edge at the surface step was calculated as:

$$E_F = (E_{(tot)} - E_{(sub)} - E_{(GNR)} + E_{F(GNR)}) / L \qquad (3)$$

where $E_{(tot)}$, $E_{(sub)}$, and $E_{(GNR)}$ are the calculated energies of the Ge-Gr edge at the Ge(110) step, stepped Ge(110) substrate, and isolated GNR respectively, $E_{F(GNR)}$ is the formation energy of GNR with a free edge, and L is the length of GNR. Owing to the C_6 symmetry of graphene, $\Delta\theta$ varies from 0 to 30°.

Limited by the size of calculation model, five different $\Delta\theta$ values were considered for each step. The optimized structures and formation energies are summaried in Supporting Information Figure S4. With regard to the Ge(110) surfaces with three typical atomic steps, the minimum formation energies are obtained at $\Delta\theta$ = 0°, suggesting that the armchair direction of the graphene island is always parallel to the [-110] direction of the Ge(110) surface regardless of the direction of atomic step on the Ge(110) surface.

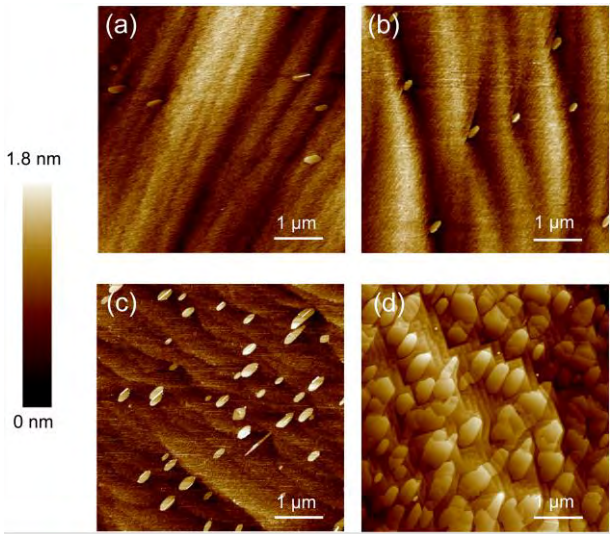

Figure S1. For the Ge(110) surface consisting of irregular atomic steps, the graphene islands are always unidirectionally aligned. Furthermore, all the aligned graphene islands are attached to the atomic steps of the substrate.

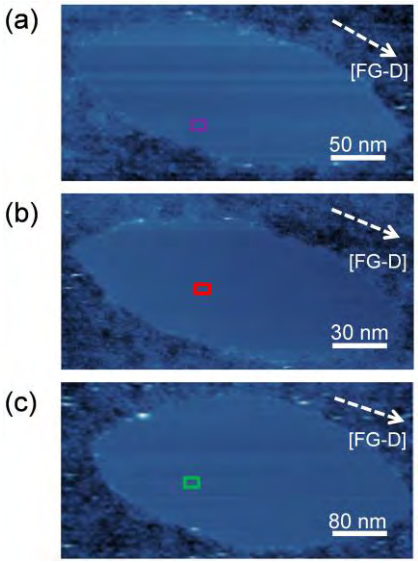

Figure S2. STM images (V = 2 V) of the single graphene island near the three representative step edges. The dashed white arrows indicate FG-Ds. The tunneling currents are (a) 1.5 nA, (b) 0.06 nA and (c) 0.2 nA, respectively. The high-resolution STM images in Figure 3 are taken from the colored rectangles, respectively. By comparing the lattice images, it can be concluded that the FG-D of graphene island coincides with the [-110] direction of the Ge(110) substrate. Therefore, based on our STM images (Figure 3) and AFM images (Figure 1d,f), the atomic steps shown in Figure 1c,d and e,f are found to be [-110] oriented and [001] oriented, respectively.

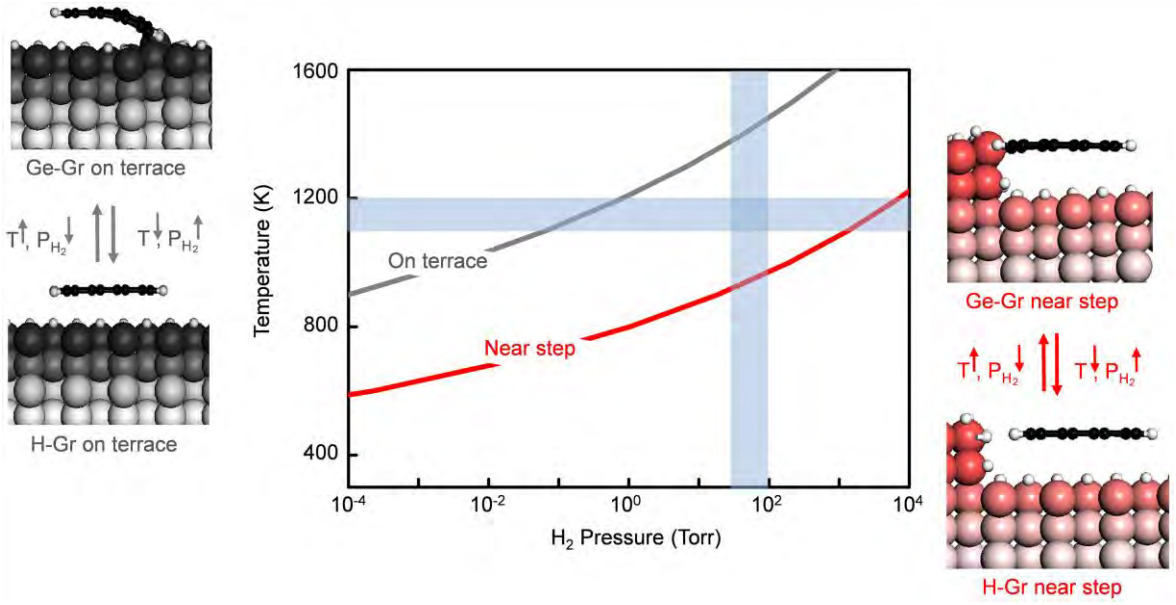

Figure S3. Thermodynamic diagram of graphene with the zigzag edge on the Ge(110) surface with terraces or [100] oriented steps. Structures for hydrogen-passivated and Ge-passivated graphene with zigzag edge on the terrace are shown in the left panel and those with zigzag edge near the [001] oriented atomic step are shown in the right panel. The hydrogen-passivated edge will be transformed into Ge-passivated one with the increase of temperature and decrease of H_2 pressure, and vice versa.

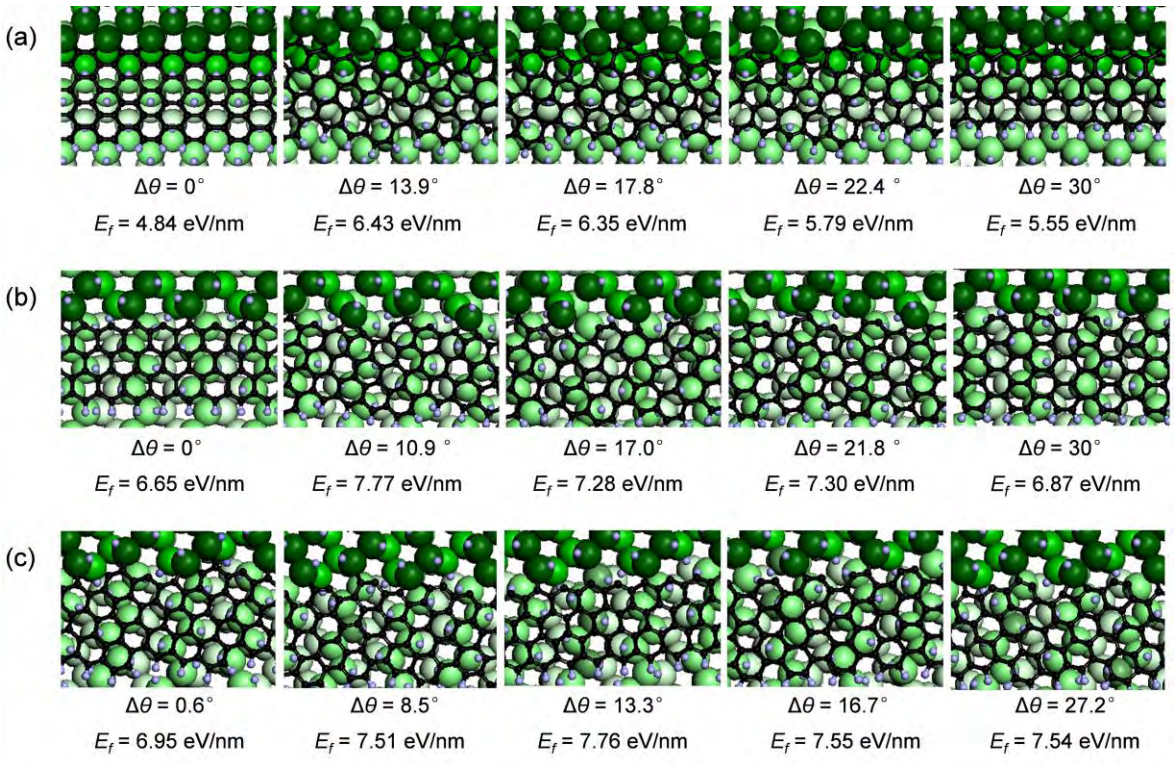

Figure S4. (a) Optimized structures and formation energies of the graphene edge attached to S-I ([-110] oriented step) with $\Delta\theta$ of 0°, 13.9°, 17.8°, 22.4° and 30°. Here, the edge of the graphene nanoribbon is used to model the graphene edge and thereafter. (b) Optimized structures and formation energies of the graphene edge attached to S-II ([001] oriented step) with $\Delta\theta$ of 0°, 10.9°, 17.0°, 21.8°, and 30°. (c) Optimized structures and formation energies of the graphene edge attached to S-III (76.74° deviated from [-110] direction) with $\Delta\theta$ of 0.6°, 8.5°, 13.3°, 16.7°, and 27.2°.

(1) Emtsev, K. V.; Bostwick, A.; Horn, K.; Jobst, J.; Kellogg, G. L.; Ley, L.; McChesney, J. L.; Ohta, T.; Reshanov, S. A.; Rohrl, J.; Rotenberg, E.; Schmid, A. K.; Waldmann, D.; Weber, H. B.; Seyller, T. *Nat. Mater.* **2009**, 8, 203-207.